

Slowly rotating black holes and their scalarization

Yun Soo Myung^{a*} and De-Cheng Zou^{b†}

^aInstitute of Basic Sciences and Department of Computer Simulation, Inje University
Gimhae 50834, Korea

^bCenter for Gravitation and Cosmology and College of Physical Science and Technology,
Yangzhou University, Yangzhou 225009, China

Abstract

We study scalarization of slowly rotating black holes in the Einstein-scalar-Gauss-Bonnet (GB)-Chern-Simons (CS) theory. In the slow rotation approximation of $a \ll 1$ with rotation parameter a , the GB term is given by a term for Schwarzschild black hole, whereas the CS term takes a linear term of a . The tachyonic instability for slowly rotating black holes represents the onset of spontaneous scalarization. We use the (2+1)-dimensional hyperboloidal foliation method to show the tachyonic instability for slowly rotating black holes by considering the time evolution of a spherically symmetric scalar mode. A threshold (existence) curve is obtained from the constant scalar modes under time evolution, which means the boundary between stable and unstable black holes. It is found that the slowly rotating black holes turn out to be unstable against a spherically symmetric scalar-mode propagation for positive coupling α . However, we could not find tachyonic instability and any a -bound for scalarization for negative coupling α .

*e-mail address: ysmyoung@inje.ac.kr

†e-mail address: dczou@yzu.edu.cn

1 Introduction

Kerr black holes were used to derive spontaneous scalarization in the Einstein-scalar-Gauss-Bonnet-scalar (EsGB) theory together with positive coupling [1, 2]. The tachyonic instability for Kerr black holes is considered as the onset of spin-induced spontaneous scalarization. Here, it is interesting to note that the sufficiently high rotations ($a \geq 0.5$) suppresses spin-induced scalarization since the GB term might become negative outside the outer horizon.

Contrastively, the sufficiently high rotations (a -bound of $a/M \geq 0.5$) enhance spin-induced scalarization for Kerr black holes in the same theory with negative coupling [3]. This a -bound was found analytically by considering an $l \rightarrow \infty$ -scalar mode [4] and numerically by solving the (2+1)-dimensional evolution equation [5]. Further, any instability was not triggered when $a < 0.5$ with $M = 1$ in the same theory [6]. Consequently, the spin-induced scalarized black holes were constructed for sufficiently high rotations in the EsGB theory with negative coupling [7, 8]. We wish to mention again that spin-induced scalarization was realized through scalar couplings to the GB term. However, we have found the threshold curve for tachyonic instability without a -bound when performing the instability analysis for Kerr black holes [9] and slowly rotating black holes [10] in the Einstein-scalar-Chern-Simons (EsCS) theory with negative coupling. This implies that the presence of a -bound represents a feature of the GB term together with negative coupling.

At this stage, it is very curious to introduce slowly rotating black holes because they do not allow for sufficiently high rotations of $a \geq 0.5$. These black holes could be obtained by confining all quantities of interest to first order in a (that is, slow rotation approximation $a \ll 1$). We would like to stress that most black holes are born very slowly rotating [11]. For example, black holes born from single stars rotate very slowly with $a = 0.01$ and fairly slow rotating black holes born from single stars are regarded as those with $a \leq 0.1$. So, we expect that scalarization of slowly rotating black holes does not require a -bound, compared to the spin-induced scalarization of Kerr black hole in the EsGB theory with negative coupling.

In this work, we will investigate the onset of scalarization for slowly rotating black holes in the Einstein-scalar-Gauss-Bonnet-Chern-Simons (EsGBCS) theory with the scalar coupling parameter α . This theory includes two single terms: the GB term being independent of a and the CS term depending on $a \cos \theta$. For our purpose, we need to introduce a setup of the numerical method. We will use the (2+1)-dimensional hyperboloidal foliation method to derive the tachyonic instability of slowly rotating black holes for positive coupling α

when choosing a spherically symmetric scalar-mode propagation. On the other hand, it may imply no tachyonic instability and thus, no a -bound for spontaneous scalarization when considering negative coupling α .

2 EsGBCS theory for slowly rotating black holes

We start with the EsGBCS theory given by

$$S = \frac{1}{16\pi} \int d^4x \sqrt{-g} \left[R - \frac{1}{2}(\partial\phi)^2 + \alpha\phi^2(R_{\text{GB}}^2 + {}^*RR) \right]. \quad (1)$$

Here we use geometric units of $G = c = 1$. We wish to describe briefly a significance of our action (1). An action including both topological terms with different linear couplings was firstly obtained from some superstring models [12] and the heterotic strings [13]. Also, we have studied spontaneous scalarization for Schwarzschild black hole in the action including both topological invariants with different quadratic couplings [14]. Inspired by these, we introduced the action (1).

In Eq. (1), the same quadratic scalar coupling function is chosen for two topological terms: the GB term

$$R_{\text{GB}}^2 = R^2 - 4R_{\mu\nu}R^{\mu\nu} + R_{\mu\nu\rho\sigma}R^{\mu\nu\rho\sigma} \quad (2)$$

and the CS term

$${}^*RR = \frac{1}{2}\epsilon^{\mu\nu\rho\sigma}R^\eta_{\xi\rho\sigma}R^\xi_{\eta\mu\nu}. \quad (3)$$

Varying (1) with respect to $g_{\mu\nu}$ and ϕ implies Einstein and scalar equations

$$G_{\mu\nu} = \frac{1}{2}\partial_\mu\phi\partial_\nu\phi - \frac{1}{4}g_{\mu\nu}(\partial\phi)^2 - 4\alpha[\nabla^\rho\nabla^\sigma(\phi^2)P_{\mu\rho\nu\sigma} + C_{\mu\nu}], \quad (4)$$

$$\nabla^2\phi + 2\alpha(R_{\text{GB}}^2 + {}^*RR)\phi = 0, \quad (5)$$

where $P_{\mu\rho\nu\sigma}$ -tensor is a divergence-free part of Riemann tensor satisfying $\nabla_\mu P^\mu_{\rho\nu\sigma} = 0$. Also, $C_{\mu\nu}$ is the Cotton tensor given by

$$C_{\mu\nu} = \nabla_\rho(\phi^2)\epsilon^{\rho\sigma\gamma}{}_{(\mu}\nabla_\gamma R_{\nu)\sigma} + \frac{1}{2}\nabla_\rho\nabla_\sigma(\phi^2)\epsilon_{(\nu}{}^{\rho\gamma\delta}R^\sigma{}_{\mu)\gamma\delta}. \quad (6)$$

Choosing $\phi = 0$, Eq. (4) reduces to $R_{\mu\nu} = 0$ which allows the Kerr spacetime as a solution written in Boyer-Lindquist coordinates

$$\begin{aligned} ds_{\text{Kerr}}^2 &\equiv \tilde{g}_{\mu\nu}dx^\mu dx^\nu \\ &= -\frac{\Delta}{\rho^2}(dt - a\sin^2\theta d\varphi)^2 + \frac{\rho^2}{\Delta}dr^2 + \rho^2 d\theta^2 + \frac{\sin^2\theta}{\rho^2}[adt - (r^2 + a^2)d\varphi]^2. \end{aligned} \quad (7)$$

Here, we have mass M , angular momentum J , rotation parameter $a = J/M > 0$, $\Delta = r^2 - 2Mr + a^2$, and $\rho^2 = r^2 + a^2 \cos^2 \theta$. It is meaningful to note that Eq. (7) describes a stationary, axisymmetric, and non-static spacetime. Considering $\Delta = 0$ leads to the outer/inner horizons as $\tilde{r}_{\pm} = M \pm \sqrt{M^2 - a^2}$.

In this case, two topological terms for Eq. (7) are given by

$$\begin{aligned} \tilde{R}_{\text{GB}}^2 &= \frac{48M^2(r^6 - 15r^4a^2 \cos^2 \theta + 15r^2a^4 \cos^4 \theta - a^6 \cos^6 \theta)}{\rho^{12}} \\ &\simeq \frac{48M^2}{r^6} \left[1 - \frac{21a^2 \cos^2 \theta}{r^2} + \dots \right], \end{aligned} \quad (8)$$

$$\begin{aligned} {}^* \tilde{R} \tilde{R} &= \frac{96rM^2a \cos \theta (3r^4 - 10r^2a^2 \cos^2 \theta + 3a^4 \cos^4 \theta)}{\rho^{12}} \\ &\simeq \frac{96M^2a \cos \theta}{r^7} \left[3 - \frac{28a^2 \cos^2 \theta}{r^2} + \dots \right]. \end{aligned} \quad (9)$$

Here \tilde{R}_{GB}^2 (${}^* \tilde{R} \tilde{R}$) is even (odd) with respect to parity transformation: $\tilde{R}_{\text{GB}}^2(\pi - \theta) = \tilde{R}_{\text{GB}}^2(\theta)$ and ${}^* \tilde{R} \tilde{R}(\pi - \theta) = -{}^* \tilde{R} \tilde{R}$. This property plays an important role in conjecturing the threshold curve for negative coupling α together with the transformation of $\alpha \rightarrow -\alpha$. Also, the second term in Eq. (8) implies that for negative α , a spherical scalar mode is stable at low rotations ($a < 0.5$) whereas it is unstable at sufficiently high rotations ($a \geq 0.5$), implying the a -bound of $a \geq 0.5$ with $M = 1$ for spin-induced scalarization in the EsGB theory [3].

Taking the slow rotation approximation ($a \ll 1$), we introduce the slowly rotating black hole keeping up to $\mathcal{O}(a)$ -order [18, 19]

$$\begin{aligned} ds_{\text{SRBH}}^2 &= \bar{g}_{\mu\nu} dx^\mu dx^\nu \\ &= - \left(1 - \frac{2M}{r} \right) dt^2 + \frac{dr^2}{1 - \frac{2M}{r}} + r^2 (d\theta^2 + \sin^2 \theta d\varphi^2) + \frac{4aM \sin^2 \theta}{r} dt d\varphi, \end{aligned} \quad (10)$$

where the last term represents the axisymmetric and non-static spacetime. Hereafter, we ignore all terms involving higher order than a in all other quantities of interest such that $\bar{R} \simeq 0$, $\bar{R}_{\mu\nu} \simeq 0$, $\bar{R}_{\mu\nu\rho\sigma} \neq 0$, \dots . In this case, the (outer) horizon is given by the Schwarzschild radius as

$$r_+ = 2M, \quad (11)$$

whereas the inner horizon ($r = r_-$) disappears. Up to $\mathcal{O}(a)$ -order, two topological terms are given by two single terms as

$$\bar{R}_{\text{GB}}^2 \simeq \frac{48M^2}{r^6} \quad (12)$$

and

$${}^* \bar{R} \bar{R} \simeq \frac{288M^2 a \cos \theta}{r^7}. \quad (13)$$

We wish to mention that Eq. (12) is just the term for the Schwarzschild black hole, while Eq. (13) is a linear term which approaches zero as $a \rightarrow 0$. It clear from Eq. (12) that there is no unstable spherical scalar mode of $l = m = 0$ for negative coupling α because the second term of $21a^2 \cos^2 \theta / r^2$ in Eq. (8) disappears. This might imply no a -bound of $a \geq 0.5$ appeared in the Kerr black hole in the EsGB theory with negative coupling α . On the other hand, considering Eq. (13), the instability of the spherical mode is determined mainly by $a \cos \theta$. This means that the rotation a plays a role in determining the instability of slowly rotating black holes, implying $\alpha > \alpha_{\text{th}}(a)$ -bound for positive coupling α . These indicate different features of two topological terms when making the slow rotation approximation. In the slow rotation approximation, the GB term provides the property of the static solution, while the CS term gives the property of non-static solution. This explains that the scalarized Schwarzschild (slowly rotating) black holes could be found from the GB (CS) coupling, but these are never found from the CS (GB) coupling.

Before we proceed, let us briefly mention the tachyonic instability on the non-rotating black holes. If $a = 0$, Eq. (10) reduces to the line element for Schwarzschild black hole (SBH)

$$\begin{aligned} ds_{\text{SBH}}^2 &= \bar{g}_{\mu\nu} dx^\mu dx^\nu \\ &= -\left(1 - \frac{2M}{r}\right) dt^2 + \frac{dr^2}{1 - \frac{2M}{r}} + r^2(d\theta^2 + \sin^2 \theta d\varphi^2). \end{aligned} \quad (14)$$

In this background, one has a linearized scalar equation

$$\left(\bar{\nabla}_{\text{SBH}}^2 + \frac{96\alpha M^2}{r^6}\right) \delta\phi = 0. \quad (15)$$

Considering

$$\delta\phi(t, r, \theta, \varphi) = \frac{u(r)}{r} e^{-i\omega t} Y_{lm}(\theta, \varphi), \quad (16)$$

and introducing a tortoise coordinate $r_* = r + 2M \ln(r/(2M) - 1)$ defined by $dr_* = dr/(1 - 2M/r)$, the radial equation of (15) leads to the Schrödinger-type equation

$$\frac{d^2 u}{dr_*^2} + \left[\omega^2 - V_{\text{SBH}}(r)\right] u(r) = 0, \quad (17)$$

where the potential $V_{\text{SBH}}(r)$ is given by

$$V_{\text{SBH}}(r) = \left(1 - \frac{2M}{r}\right) \left[\frac{2M}{r^3} + \frac{l(l+1)}{r^2} - \frac{96\alpha M^2}{r^6} \right]. \quad (18)$$

In the case of $s(l=0)$ -mode, from $\int_{2M}^{\infty} dr V_{\text{SBH}}(r)/(1-2M/r) < 0$, we obtain a sufficient condition of an unstable bound on the coupling parameter α [15]

$$\alpha_{\text{sc}}^{l=0} > 0.4167M^2. \quad (19)$$

However, (19) is not a necessary and sufficient condition for instability. In order to determine the tachyonic instability precisely, one has to solve the second-order differential equation numerically

$$\frac{d^2 u}{dr_*^2} - \left[\Omega^2 + V_{\text{SBH}}(r) \right] u(r) = 0, \quad (20)$$

which may allow an exponentially growing mode of $e^{\Omega t}$ ($\omega = i\Omega$) as an unstable mode. Here we choose two boundary conditions: a normalizable solution of $u(\infty) \sim e^{-\Omega r_*}$ at infinity and a solution of $u(2M) \sim (r-2M)^{2M\Omega}$ near the horizon. Actually, the bound for tachyonic instability is less than (19) and given by $\alpha \geq 0.3628$ with $M = 1$. This shows that small $\alpha < 0.3628$ is not enough to trigger the tachyonic instability. The unstable region will be represented by a red-line on the α -axis in the GBCS-threshold curve. The spontaneous scalarization of SBH was studied in the EsGB theory [15, 16, 17] and the EsGBCS theory [14].

Finally, we would like to mention that the $s(l=0)$ -mode analysis is not enough to deduce stability/instability because the analysis for higher mode with $l \geq 1$ is necessary to be performed. In this case, from (18), there exists a positive contribution of $l(l+1)/r^2$ to the potential with $l = 0$. It is worth noting that V_{SBH} with $l \geq 1$ indicates potential barrier [see (Left) Fig. 1] for fixed $\alpha = 0.6$, whereas it shows potential well in the near horizon [see (Right) Fig. 1] with $\alpha \geq 0.6$ for fixed l . This implies that the $l = 1$ -mode may be stable even for the unstable region ($\alpha \geq 0.3628$) of the $l = 0$ mode. We note that the shapes of potential V_{SBH} with $l = 0$ for $\alpha \leq 0.5$ are similar to (Right) Fig. 1. Analytically, the sufficient condition for instability could be derived from $\int_{2M}^{\infty} dr V_{\text{SBH}}(r)/(1-2M/r) < 0$ as

$$\alpha_{\text{sc}}^l > 0.4168 + 0.8333l(l+1), \quad (21)$$

which means that increasing l makes increasing α -bound. Explicitly, it implies for $l = 1$

$$\alpha_{\text{sc}}^{l=1} > 2.0833, \quad (22)$$

which is large than the lowest bound of $l = 0$ given by (19).

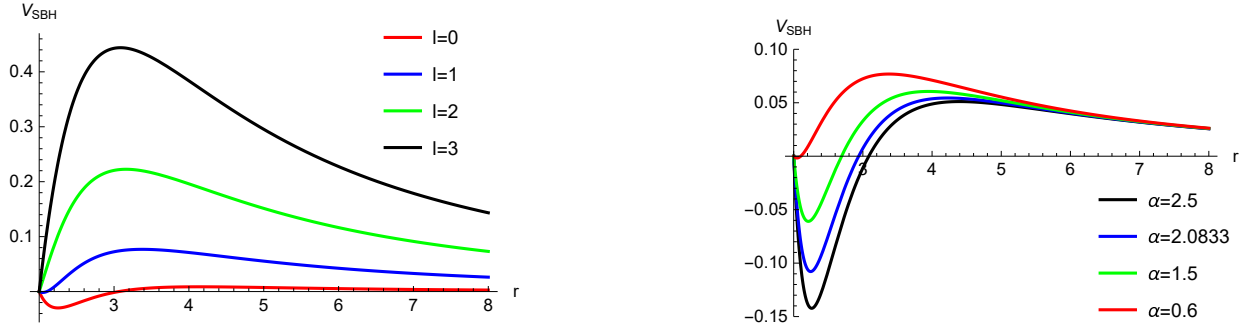


Figure 1: Potentials V_{SBH} around SBH: (Left) V_{SBH} with different l for fixed $\alpha = 0.6$. (Right) V_{SBH} with different α for fixed $l = 1$, showing potential wells in the near horizon. Here we choose $M = 1$.

3 Unstable slowly rotating black holes

To explore the onset of scalarization for slowly rotating black holes, the perturbations $(h_{\mu\nu}, \delta\phi)$ propagating around the slowly rotating black hole background are introduced as

$$g_{\mu\nu} = \bar{g}_{\mu\nu} + h_{\mu\nu}, \quad \phi = \bar{\phi} + \delta\phi \quad \text{with } \bar{\phi} = 0. \quad (23)$$

The linearized equation to (4) takes a simple form like the general relativity as

$$\delta R_{\mu\nu}(h) \simeq 0, \quad (24)$$

where

$$\delta R_{\mu\nu}(h) = \frac{1}{2} (\bar{\nabla}^\gamma \bar{\nabla}_\mu h_{\nu\gamma} + \bar{\nabla}^\gamma \bar{\nabla}_\nu h_{\mu\gamma} - \bar{\nabla}^2 h_{\mu\nu} - \bar{\nabla}_\mu \bar{\nabla}_\nu h). \quad (25)$$

The linearized scalar equation is important to test the stability of slowly rotating black holes and it is given by

$$\left(\bar{\nabla}^2 - \mu_{\text{eff}}^2 \right) \delta\phi = 0 \quad (26)$$

with an effective mass composed of two terms

$$\mu_{\text{eff}}^2 \equiv \mu_{\text{GB}}^2 + \mu_{\text{CS}}^2 = -2\alpha \bar{R}_{\text{GB}}^2 - 2\alpha^* \bar{R} \bar{R}(a). \quad (27)$$

It is helpful to note that a tensor-stability analysis for the slowly rotating black hole with Eq. (24) is the same as in the general relativity. One might not find unstable tensor modes



Figure 2: 3D graphs of μ_{eff}^2 for $a=0.05$ with positive α (Left) and $a=0.05$ with negative α (Right) including $r \in [r_+ = 2, 5]$ and $\theta \in [0, \pi]$. The red, green, and blue surfaces represent $\alpha = \pm 0.3, \pm 0.4$ and ± 1.0 , respectively. For positive α (Left), the potential wells are deeper and deeper as α increases while the potential barriers are higher and higher as $-\alpha$ increases for negative α (Right).

propagating around the slowly rotating black hole background [20]. Hence, the stability of slowly rotating black hole will be determined totally by the linearized scalar equation (26) in the EsGBCS theory. We remind the reader that $\mu_{\text{GB}}^2(\mu_{\text{CS}}^2)$ is variant (invariant) under a combined transformation of $\alpha \rightarrow -\alpha$ and $\theta \rightarrow \pi - \theta$ [21]. From now on, we consider the case of $\alpha > 0$.

We find from Eqs. (12) and (13) that \bar{R}_{GB}^2 is always positive and decreasing with r (being independent of a), while ${}^* \bar{R} \bar{R}(a)$ is an odd function with respect to $\cos \theta$. We observe from (Left) Fig. 2 that μ_{eff}^2 indicates negative regions outside the horizon. The potential wells are deeper and deeper as α increases. It seems that these may provide the tachyonic instability. At this stage, we note that small negative $\mu_{\text{eff}}^2|_{\alpha=0.3}$ is not sufficient to trigger the tachyonic instability whereas large negative $\mu_{\text{eff}}^2|_{\alpha=1}$ is sufficient to trigger the tachyonic instability. On the other hand, from (Right) Fig. 2, the negative α case suggests positive regions outside the horizon, implying no instability. However, the above is a rough estimation to see the instability even for positive α because μ_{eff}^2 depends α as well as a . We note that the threshold curve $\alpha_{\text{th}}(a)$ for slowly rotating black holes depends on a . It will be determined precisely by carrying out numerical computations. As an example, after computing the threshold of instability $\alpha_{\text{th}}(a = 0.05) = 0.3627$, we know that it is stable for $\alpha(= 0.3) < \alpha_{\text{th}}$ while it is unstable for $\alpha(= 0.4, 1) > \alpha_{\text{th}}$.

Let us briefly mention the (2+1)-dimensional hyperboloidal foliation method to solve Eq.

(26) numerically [22]. Firstly, we introduce the ingoing Kerr-Schild coordinates $\{\tilde{t}, r, \theta, \tilde{\varphi}\}$ by considering the coordinate transformations

$$d\tilde{t} = dt + \frac{2Mr}{\Delta}dr, \quad d\tilde{\varphi} = d\varphi + \frac{a}{\Delta}dr. \quad (28)$$

Considering separation of variables

$$\delta\phi(\tilde{t}, r, \theta, \tilde{\varphi}) = \frac{1}{r} \sum_m u_m(\tilde{t}, r, \theta) e^{im\tilde{\varphi}}, \quad (29)$$

Eq.(26) leads to a (2+1)-dimensional Teukolsky equation as

$$A^{\tilde{t}\tilde{t}}\partial_{\tilde{t}}^2 u_m + A^{\tilde{t}r}\partial_{\tilde{t}}\partial_r u_m + A^{rr}\partial_r^2 u_m + A^{\theta\theta}\partial_{\theta}^2 u_m + B^{\tilde{t}}\partial_{\tilde{t}} u_m + B^r\partial_r u_m + B^{\theta}\partial_{\theta} u_m + C u_m = 0 \quad (30)$$

with coefficients

$$\begin{aligned} A^{\tilde{t}\tilde{t}} &= \rho^2 + 2Mr, & A^{\tilde{t}r} &= -4Mr, & A^{rr} &= -\Delta, & A^{\theta\theta} &= -1, \\ B^{\tilde{t}} &= 2M, & B^r &= \frac{2}{r}(a^2 - Mr) - 2ima, & B^{\theta} &= -\cot\theta, \\ C &= \frac{m^2}{\sin^2\theta} - \frac{2(a^2 - Mr)}{r^2} + \frac{2ima}{r} + \mu_{\text{eff}}^2 \rho^2. \end{aligned} \quad (31)$$

As the second step, we wish to solve Eq. (30) by adopting the hyperboloidal foliation method [23] with compactified horizon-penetrating hyperboloidal (HH) coordinates $\{\tau, \rho, \theta, \tilde{\varphi}\}$. In this case, Eq. (30) could be rewritten as

$$\partial_{\tau}^2 u_m = \tilde{A}^{\tau\rho}\partial_{\tau}\partial_{\rho} u_m + \tilde{A}^{\rho\rho}\partial_{\rho}^2 u_m + \tilde{A}^{\theta\theta}\partial_{\theta}^2 u_m + \tilde{B}^{\tau}\partial_{\tau} u_m + \tilde{B}^{\rho}\partial_{\rho} u_m + \tilde{B}^{\theta}\partial_{\theta} u_m + \tilde{C} u_m = 0, \quad (32)$$

where coefficients appeared in [6]. Finally, introducing a momentum Π_m , one finds two coupled first-order equations as

$$\partial_{\tau} u_m = \Pi_m, \quad (33)$$

$$\partial_{\tau} \Pi_m = \tilde{B}^{\tau}\Pi_m + \tilde{A}^{\tau\rho}\partial_{\rho}\Pi_m + \tilde{A}^{\rho\rho}\partial_{\rho}^2 u_m + \tilde{A}^{\theta\theta}\partial_{\theta}^2 u_m + \tilde{B}^{\rho}\partial_{\rho} u_m + \tilde{B}^{\theta}\partial_{\theta} u_m + \tilde{C} u_m. \quad (34)$$

The ρ and θ -differential equations are solved by using the finite difference method, whereas the time (τ) evolution is obtained by applying the fourth-order Runge-Kutta integrator. Using the HH coordinates leads to the fact that the ingoing (outgoing) boundary conditions at the horizon (infinity) are satisfied automatically. Furthermore, the boundary conditions at the poles are given as $u_m|_{\theta=0,\pi} = 0$ for odd m and $\partial_{\theta} u_m|_{\theta=0,\pi} = 0$ for even m .

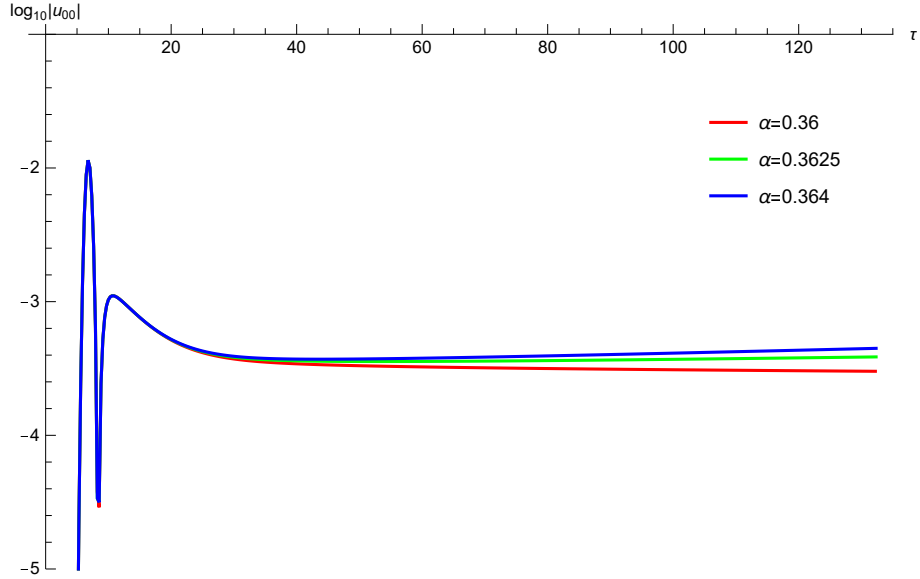


Figure 3: Time evolution of a scalar mode $\log_{10} |u_{00}(\tau, \rho = 6M, \alpha)|$ for $a = 0.15$ with three different α . $\alpha = 0.36$ represents stability (\searrow), $\alpha = 0.3625$ denotes threshold (\longrightarrow), and $\alpha = 0.364$ represents instability (\nearrow). The middle curve represents the threshold point at $a = 0.15$ in Fig. 4.

One introduces a Gaussian function $[u_{lm}(\tau = 0, \rho, \theta) \sim Y_{lm}(\theta)e^{-\frac{(\rho-\rho_c)^2}{2\sigma^2}}]$ localized at $\rho = \rho_c$ outside the horizon as an initial data for u_{lm} . In addition, we may have an initial boundary condition of $\Pi_{lm}(\tau = 0, \rho, \theta) = 0$ if Eq. (33) holds at $\tau = 0$. Here, we take $\rho_c = 6M$ with $M = 1$. Observers are assumed to be located at $\rho = 6M$ and $\theta = \pi/4$.

The mode coupling may occur because the slowly rotating spacetime is not spherically symmetric. This implies that different l -modes with the same m are not independent and thus, coupled to each other. However, it is suggested that the $l = m$ will become dominant. As an example, the late-time dominant mode is the mode with $l = m = 0$ among the processes starting with $l = 0, 1, 2$ and $m = 0$ [22]. This means that the $l = m = 0$ case is always a dominant mode whatever the initial mode is chosen. Concerning the range for a , we confine ourselves to $0 \leq a \leq 0.3$ including fairly slow rotating black holes ($0 \leq a \leq 0.1$) because we are considering the slowly rotating black holes. Also, we expect that the GBCS-threshold curve $\alpha = \alpha_{\text{th}}(a)$ being the boundary between stable and unstable black holes may exist around $\alpha = 0.3628$ because \bar{R}_{GB}^2 in (12) is dominant in the slow rotating approximation.

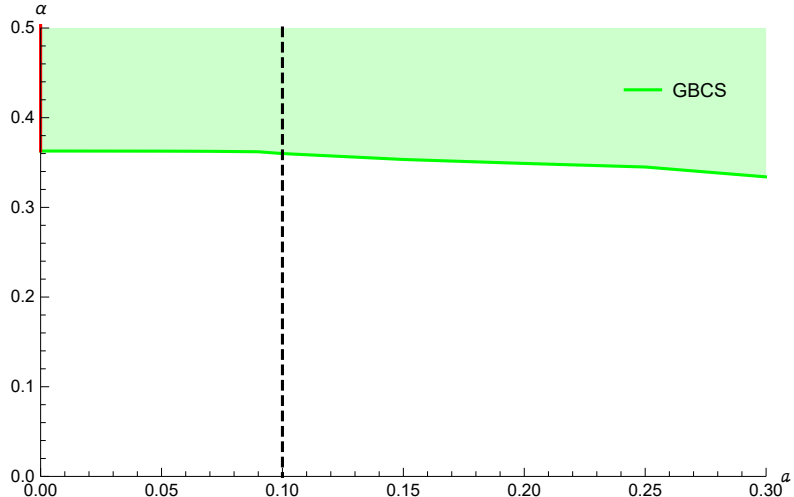


Figure 4: GBCS-threshold (existence) curve $\alpha = \alpha_{\text{th}}(a)$ being the boundary between stable and unstable slowly rotating black holes is obtained from observing time evolution of $l = m = 0$ -scalar mode for positive α . The dashed line denotes the upper limit for fairly slow rotating black holes ($0 < a \leq 0.1$). Also, it includes the stable and unstable (red-line: $\alpha \geq 0.3628$) Schwarzschild black holes on the α -axis found from the GB term only.

Here, we take a spherically symmetric mode of $l = m = 0$ as an initial mode. As is shown Fig. 3, the time evolution for $\log_{10} |u_{00}(\tau, \rho = 6M, \alpha)|$ provides stability (\searrow), threshold (\longrightarrow), and instability (\nearrow) with increasing time (τ).

From Fig. 4, we find a threshold curve $\alpha = \alpha_{\text{th}}(a)$ which is the boundary between stable and unstable black holes based on the constant scalar modes [$\log_{10} |u_{00}(\tau, \rho, \alpha)| \sim \longrightarrow$]. We observe that the GBCS-threshold curve decreases very slowly as a increases and it hits the α -axis at $\alpha = 0.3628$ when $a = 0$. The region for fairly slow rotating black holes denotes $0 < a \leq 0.1$ and the upper limit is represented by a dashed line at $a = 0.1$. The unshaded lower region [$\alpha < \alpha_{\text{th}}(a)$: no growing mode] represents stable slowly rotating black holes, while the shaded upper region [$\alpha \geq \alpha_{\text{th}}(a)$: growing mode] denotes the unstable slowly rotating black holes. Also, Fig. 4 includes stable ($\alpha < 0.3628$) and unstable (red-line: $\alpha \geq 0.3628$) Schwarzschild black holes on the α -axis which is derived from the GB term solely. If one uses either $l = m = 1$ or $l = m = 2$ as initial modes, the stable region (unshaded lower region) will be increased, compared to the $l = m = 0$ case.

At this stage, we consider the case with negative coupling α . In this case, there is no tachyonic instability for scalarization because μ_{eff}^2 has positive region outside the horizon for

negative α (see (Right) Fig. 2). Also, this implies the absence of a -bound for spontaneous scalarization.

Finally, we would like to mention the superradiant instability, which is known to exist at high rotations for constant real masses [24, 25, 26, 27]. Further, superradiance appears if bosonic waves with angular momentum are amplified when scattered by a spinning black hole, which spins down the black hole. Superradiant scattering could develop into an instability since the bosonic field is confined near the black hole by its constant mass. It is worth noting that superradiant instability may occur with nonconstant effective mass [28]. In our work, however, the tachyonic instability is more plausible to occur than superradiant instability because rapid falloffs of (12) and (13) are present [3]. More precisely, this is because (12) and (13) make a potential well but not a potential shape with barrier-well-mirror which provides quasibound states for superradiant instability [25, 29].

4 Discussions

It is very curious to note that most black holes born from single stars rotate slowly. We have performed spontaneous scalarization of slowly rotating black holes in the EsGBCS theory. The fairly slow rotating black holes represent the cases with $0 < a \leq 0.1$ [11]. In the slow rotation approximation with $a \ll 1$, the GB term is a larger term for Schwarzschild black hole while the CS term takes a smaller linear term of a -rotation parameter, implying that its tachyonic instability is determined mainly by the GB term. The tachyonic instability for slowly rotating black holes implies the onset of spontaneous scalarization.

The (2+1)-dimensional hyperboloidal foliation method is used to show the tachyonic instability of slowly rotating black holes when considering a spherically symmetric scalar-mode propagation u_{00} . The time evolution for $\log_{10} |u_{00}(\tau, \rho, \alpha)|$ indicates stability (\searrow), threshold (\longrightarrow), and instability (\nearrow) with increasing time (τ) shown in Fig. 3. It is shown that slowly rotating black holes are unstable against a spherically symmetric scalar-mode of $l = m = 0$ for positive coupling α only. To this end, we have constructed a threshold curve $\alpha = \alpha_{\text{th}}(a)$ in Fig. 4 which is the boundary between stable and unstable black holes based on the constant scalar modes [$\log_{10} |u_{00}(\tau, \rho, \alpha)| \sim \longrightarrow$].

For negative coupling, there is no tachyonic instability for scalarization since μ_{eff}^2 has positive region outside the horizon. Additionally, we could not find the a -bound for spin-

induced scalarization obtained from the Kerr black hole in the EsGB theory. However, we propose that the a -bound for spin-induced scalarization of Kerr black holes will be shifted from $a \geq 0.5$ to a lower bound due to the CS term in the EsGBCS theory with negative coupling [30].

Acknowledgments

This work was supported by the National Research Foundation of Korea (NRF) grant funded by the Korea government (MOE) (No. NRF-2017R1A2B4002057).

References

- [1] P. V. P. Cunha, C. A. R. Herdeiro and E. Radu, *Phys. Rev. Lett.* **123**, no. 1, 011101 (2019) doi:10.1103/PhysRevLett.123.011101 [arXiv:1904.09997 [gr-qc]].
- [2] L. G. Collodel, B. Kleihaus, J. Kunz and E. Berti, *Class. Quant. Grav.* **37**, no. 7, 075018 (2020) doi:10.1088/1361-6382/ab74f9 [arXiv:1912.05382 [gr-qc]].
- [3] A. Dima, E. Barausse, N. Franchini and T. P. Sotiriou, *Phys. Rev. Lett.* **125**, no. 23, 231101 (2020) doi:10.1103/PhysRevLett.125.231101 [arXiv:2006.03095 [gr-qc]].
- [4] S. Hod, *Phys. Rev. D* **102**, no. 8, 084060 (2020) doi:10.1103/PhysRevD.102.084060 [arXiv:2006.09399 [gr-qc]].
- [5] D. D. Doneva, L. G. Collodel, C. J. Krüger and S. S. Yazadjiev, *Phys. Rev. D* **102**, no. 10, 104027 (2020) doi:10.1103/PhysRevD.102.104027 [arXiv:2008.07391 [gr-qc]].
- [6] S. J. Zhang, B. Wang, A. Wang and J. F. Saavedra, *Phys. Rev. D* **102**, no. 12, 124056 (2020) doi:10.1103/PhysRevD.102.124056 [arXiv:2010.05092 [gr-qc]].
- [7] C. A. R. Herdeiro, E. Radu, H. O. Silva, T. P. Sotiriou and N. Yunes, *Phys. Rev. Lett.* **126**, no. 1, 011103 (2021) doi:10.1103/PhysRevLett.126.011103 [arXiv:2009.03904 [gr-qc]].
- [8] E. Berti, L. G. Collodel, B. Kleihaus and J. Kunz, *Phys. Rev. Lett.* **126**, no. 1, 011104 (2021) doi:10.1103/PhysRevLett.126.011104 [arXiv:2009.03905 [gr-qc]].
- [9] Y. S. Myung and D. C. Zou, *Phys. Lett. B* **814**, 136081 (2021) doi:10.1016/j.physletb.2021.136081 [arXiv:2012.02375 [gr-qc]].
- [10] Y. S. Myung and D. C. Zou, arXiv:2103.01389 [gr-qc].
- [11] J. Fuller and L. Ma, *Astrophys. J. Lett.* **881**, no. 1, L1 (2019) doi:10.3847/2041-8213/ab339b [arXiv:1907.03714 [astro-ph.SR]].
- [12] I. Antoniadis, J. Rizos and K. Tamvakis, *Nucl. Phys. B* **415**, 497 (1994) doi:10.1016/0550-3213(94)90120-1 [hep-th/9305025].

- [13] P. A. Cano and A. Ruipérez, JHEP **1905**, 189 (2019) Erratum: [JHEP **2003**, 187 (2020)] doi:10.1007/JHEP05(2019)189, 10.1007/JHEP03(2020)187 [arXiv:1901.01315 [gr-qc]].
- [14] Y. S. Myung and D. C. Zou, Int. J. Mod. Phys. D **28**, no. 09, 1950114 (2019) doi:10.1142/S0218271819501141 [arXiv:1903.08312 [gr-qc]].
- [15] D. D. Doneva and S. S. Yazadjiev, Phys. Rev. Lett. **120**, no. 13, 131103 (2018) doi:10.1103/PhysRevLett.120.131103 [arXiv:1711.01187 [gr-qc]].
- [16] H. O. Silva, J. Sakstein, L. Gualtieri, T. P. Sotiriou and E. Berti, Phys. Rev. Lett. **120**, no. 13, 131104 (2018) doi:10.1103/PhysRevLett.120.131104 [arXiv:1711.02080 [gr-qc]].
- [17] G. Antoniou, A. Bakopoulos and P. Kanti, Phys. Rev. Lett. **120**, no. 13, 131102 (2018) doi:10.1103/PhysRevLett.120.131102 [arXiv:1711.03390 [hep-th]].
- [18] J. Lense and H. Thirring, Phys. Z. **19**, 156 (1918).
- [19] C. Lämmerzahl, M. Maceda and A. Macías, Class. Quant. Grav. **36**, no. 1, 015001 (2019) doi:10.1088/1361-6382/aaeca7 [arXiv:1802.03766 [gr-qc]].
- [20] D. Hafner, P. Hintz and A. Vasy, arXiv:1906.00860 [math.AP].
- [21] S. J. Zhang, arXiv:2102.10479 [gr-qc].
- [22] Y. X. Gao, Y. Huang and D. J. Liu, Phys. Rev. D **99**, no. 4, 044020 (2019) doi:10.1103/PhysRevD.99.044020 [arXiv:1808.01433 [gr-qc]].
- [23] I. Racz and G. Z. Toth, Class. Quant. Grav. **28**, 195003 (2011) doi:10.1088/0264-9381/28/19/195003 [arXiv:1104.4199 [gr-qc]].
- [24] T. Damour, N. Deruelle and R. Ruffini, Lett. Nuovo Cim. **15**, 257 (1976). doi:10.1007/BF02725534
- [25] T. J. M. Zouros and D. M. Eardley, Annals Phys. **118**, 139 (1979). doi:10.1016/0003-4916(79)90237-9
- [26] S. L. Detweiler, Phys. Rev. D **22**, 2323 (1980). doi:10.1103/PhysRevD.22.2323

- [27] S. R. Dolan, Phys. Rev. D **76**, 084001 (2007) doi:10.1103/PhysRevD.76.084001 [arXiv:0705.2880 [gr-qc]].
- [28] A. Dima and E. Barausse, Class. Quant. Grav. **37**, no. 17, 175006 (2020) doi:10.1088/1361-6382/ab9ce0 [arXiv:2001.11484 [gr-qc]].
- [29] A. Arvanitaki and S. Dubovsky, Phys. Rev. D **83**, 044026 (2011) doi:10.1103/PhysRevD.83.044026 [arXiv:1004.3558 [hep-th]].
- [30] D. C. Zou and Y. S. Myung, Phys. Lett. B **820**, 136545 (2021) doi:10.1016/j.physletb.2021.136545 [arXiv:2104.06583 [gr-qc]].